Barrios-Gumiel, A. et al. (2020) 'Effect of PEGylation on the biological properties of cationic carbosilane dendronized gold nanoparticles', International journal of pharmaceutics, 573, pp. 118867–118867.

Available at https://doi.org/10.1016/j.ijpharm.2019.118867

Effect of PEGylation on the biological properties of cationic carbosilane dendronized gold nanoparticles

Andrea Barrios-Gumiel,[1,2,3] Javier Sánchez-Nieves,[1,2,3] Elzbieta Pedziwiatr-Werbicka,[4,*] Viktar Abashkin,[5] Natallia Shcharbina,[6] Dzmitry Shcharbin,[5] Sława Glińska,[7] Karol Ciepluch,[8] Dorota Kuc-Ciepluch,[8] Dominika Lach,[4] Maria Bryszewska,[4] Rafael Gómez,[1,2,3,*] F. Javier de la Mata[1,2,3,*]

[1] Dpto. de Química Orgánica y Química Inorgánica. Universidad de Alcalá (UAH). Campus Universitario. E-28871 Alcalá de Henares (Madrid) Spain. Instituto de Investigación Química "Andrés M. del Río" (IQAR). Universidad de Alcalá (UAH).

[2] Networking Research Center for Bioengineering. Biomaterials and Nanomedicine (CIBER-BBN), Spain.

[3] Instituto Ramón y Cajal de Investigación Sanitaria, IRYCIS, Spain.

[4] University of Lodz, Faculty of Biology and Environmental Protection, Department of General Biophysics, 141/143 Pomorska Street, 90-236 Lodz, Poland; elzbieta.pedziwiatr@biol.uni.lodz.pl.

[5] Institute of Biophysics and Cell Engineering of NASB, Minsk, Belarus; shcharbin@gmail.com.

[6] Clinical Unit "Eleous" at Religious community «All Saints Parish in Minsk Eparchy of Belarusian Orthodox Church», Minsk, Belarus; nata.shcharbina@mail.ru.

[7] University of Lodz, Faculty of Biology and Environmental Protection, Laboratory of Microscopic Imaging and Specialized Biological Techniques, Banacha 12/16, 90-237 Lodz, Poland; slawa.glinska@biol.uni.lodz.pl.

[8] Department of Biochemistry and Genetics, Jan Kochanowski Universit, Świętokrzyska Street 15, 25-406 Kielce, Poland.

ABSTRACT

Heterofunctionalized gold nanoparticles (AuNP) were obtained in a one pot reaction of gold precursor with cationic carbosilane dendrons (first to third generations, 1-3G) and (polyethylene)glycol (PEG) ligands in the presence of a reducing agent. The final dendron/PEG proportion on AuNPs depends on the initial dendron/PEG ratio (3/1, 1/1, 1/3) and dendron generation. AuNPs were characterized by transmission electron microscopy (TEM), dynamic light scattering (DLS), ultraviolet spectroscopy (UV-VIS), thermogravimetric analysis (TGA), nuclear magnetic resonance (^{1}H-NMR) and zeta potential (ZP). Several assays have been carried out to determine the relevance of PEG/dendron ratio and dendron generation in the biomedical properties of PEGylated AuNPs and the results have been compared with those obtained for non-PEGylated AuNPs. Finally, analyses of PEG recognition by anti-PEG antibodies were carried out. In general, haemolysis, platelet aggregation and toxicity were reduced after PEGylation of AuNPs, the effect being dependent on dendron generation and dendron/PEG ratio. Dendron generation determines the exposure of PEG ligand and the interaction of this ligand with AuNPs environment. On the other hand, increasing PEG proportion diminishes toxicity but also favors interaction with antibodies.

Keywords: gold nanoparticles, carbosilane dendron, PEG, toxicity, haemolysis, platelets aggregation, PEG-antibody.

INTRODUCTION

The design of carriers for biomedicine is an outstanding tool that pretends finding versatile systems to deliver biomacromolecules or drugs.[1-5] The goals of carries are to protect bioactive systems from degradation, to increase circulation time and solubility and, if possible, to guide biomacromolecules or drugs to a specific target. The transporting of these systems can be done through different approaches, being one of them formation of electrostatic complexes. This option is widely used for nucleic acid delivery, since its polyanionic nature favors formation of complexes with polycationic systems.[6, 7] Also, this approach can be used for proteins or peptides, which contain charge domains of different nature, and drugs.[7-14]

One strategy to design carriers makes use of the enhance stability achieved with polyfunctional compounds, due to establishment of multiple interactions that mimics the behavior observed in biomacromolecules.[15-17] To this end, several type of artificial polyfunctional macromolecules have been developed: metal and metal oxide nanoparticles (NP), soft nanoparticles, polymers, dendrimers, liposomes, etc.[1, 7, 18, 19]

For example, the unique properties of metal NP, such as small size, high surface area, ease of functionalization, associated to properties of gold, such as biocompatibility, low toxicity and high stability, make gold nanoparticles (AuNP) ideal for several biomedical applications, including as carriers.[20-25]

Other type of systems deeply studied as carriers of different active biomacromolecules are dendritic systems (dendrimers and dendrons).[18, 26, 27] These multivalent molecules are built following iterative reactions leading to well-defined hyperbranched structures. This fact allows for establishing structure/activity relationships easily, in comparison with traditional polymers. Several types of dendrimers have been developed, e.g. poly(amidoamine) (PAMAM), polypropilenimine

(PPI), phosphorus dendrimers, carbosilane dendrimers. They differ mainly on the heteroatoms that compose their framework, which have huge influence on their hydrophilic/hydrophobic character. In the particular case of carbosilane dendrimers, their inner structure is clearly hydrophobic. However, if their surface is covered with cationic groups they have shown good behavior as carriers,[28, 29] being even able to cross the blood brain barrier.[30, 31]

Additionally, dendrimers and dendrons can stabilize AuNPs through terminal groups of dendrimers or by anchoring dendrons on the surface of the NPs through the focal point.[32-35] If these dendronized NPs are decorated with the corresponding cationic groups, they can also serve as carriers.[36-38]

Carriers injected in blood current will interact with a diversity of cells (e. g. red blood cells, lymphocites) and distributed through the body.[39] Therefore, the analyses of their biological properties are prioritary.[40-42] It is important to note that the cationic charges, which are responsible of stabilizing the complexes between catinionic macromolecules and nucleic acids (nanoplexes), are also responsible of the toxicity of these systems.[43] Hence, several strategies to reduce toxicity have been developed: synthesis of degradable systems, hiding of cationic charge, introducing biocompatible ligands as polyethylenglycol (PEG), etc.[13, 44]

In the particular case of PEG, it is widely used to camouflage carriers from non-desired interactions in a biological environment, favoring also solubility and biocompatibility (process known as PEGylation).[45-48] The hydrophilic nature of PEG favors formation of a hydration sphere that surrounds the nanocarriers. This steric shield protects the charge surface from interaction with blood components and other carriers, increasing also circulation time.[49, 50] Particularly, PEGylation of NPs and dendrimers reduces hemolysis[51-53] and interaction with several blood proteins.[54, 55] Unfortunately,

this widespread strategy has also its own problems such as making difficult cellular absorption or production of antibodies by the immune system that specifically recognize PEG. These difficulties lead to loss of efficacy and appearance of adverse effects as allergy reactions.[56-60]

Previously, we have described AuNPs covered with cationic dendrons that were tested for gene delivery. However, their toxicity prevented the use of higher generation systems and the transfection efficiency was low.[37] With the aim to improve their biological properties, herein we report the synthesis of AuNPs covered with cationic carbosilane dendrons of three different generations and PEG ligands. Several dendron/PEG ratios have been employed with the aim to determine the influence of dendron generation and dendron/PEG ratios on the biological properties of these PEGylated AuNPs. These systems have been fully characterized through different techniques. Biological assays to test their potential as vehicles for delivery of nucleic acids or drugs have been carried out: haemolysis, toxicity, platelet aggregation, cellular uptake, recognition by PEG antibodies.

RESULTS AND DISCUSSION

Synthesis and characterization of gold nanoparticles (AuNPs)

For simplicity, the following nomenclature will be used to name dendrons described in this work: XG_nY_m, where 'X' represents the focal point, 'G_n', carbosilane dendron generation, 'Y' denotes nature of peripheral groups and "m" the number of these groups.

For preparation of bifunctionalized AuNPs, we have employed two ligands containing a thiol moiety: the cationic dendrons $HSG_n(S\text{-}NMe_3^+)_m$ (n = 1, m = 2 (**I**); n = 2, m = 4 (**II**); n = 3, m = 8 (**III**), see Figure S1)[37] and a commercial

(polyethylene)glycol (PEG) ligand ($CH_3O(CH_2CH_2O)_nCH_2CH_2SH$, HS-PEG, M_n = 800). These new AuNPs were synthesized in water by the direct reaction of $HAuCl_4 \cdot 3H_2O$ with a mixture of both thiol derivatives and $NaBH_4$ as reducing agent. To evaluate the influence of PEG ligand on physical and biomedical properties of these new AuNPs, three different dendron/PEG ratios (3/1, 1/1, 1/3) were used (Scheme 1). The AuNPs thus obtained are named as N_mAuNP; where 'N' represents the carbosilane dendron generation (1-3) and 'm' represents the dendron/PEG ratio (a = 3/1, b = 1/1, c = 1/3). Related homofunctionalized AuNPs follow the same nomenclature without letter 'm': NAuNP. The heterofunctionalized AuNPs (**1a-cAuNP**, **2a-cAuNP**, **3a-cAuNP**) were produced in high yield as black solids soluble in water. This methodology is a straightforward procedure to prepare metal NPs with different ligands, reducing the amount of ligands with respect to the indirect or substitution procedure.[35] Heterofunctionalized AuNPs **1-3,a-cAuNPs** were characterized by transmission electron microscopy (TEM), dynamic light scattering (DLS), ultraviolet spectroscopy (UV-VIS), thermogravimetric analysis (TGA), nuclear magnetic resonance (^{1}H-NMR) and zeta potential (ZP) (Table 1, Table S1).

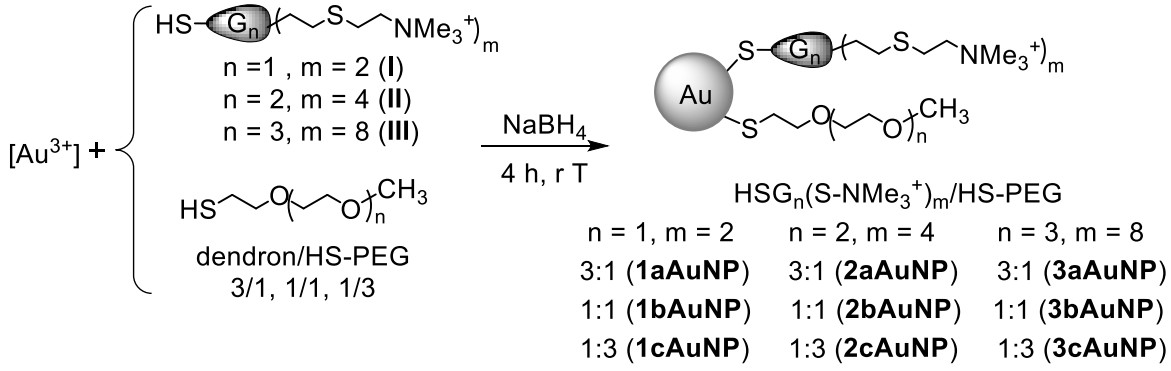

Scheme 1. Synthesis of heterofunctionalized AuNPs (n = 1, m = 2 (**1a-cAuNP**); n = 2, m = 4 (**2a-cAuNP**); n = 3, m = 8 (**3a-cAuNP**). Figure S1 depicts full structure of dendrons **I-III**.[37]

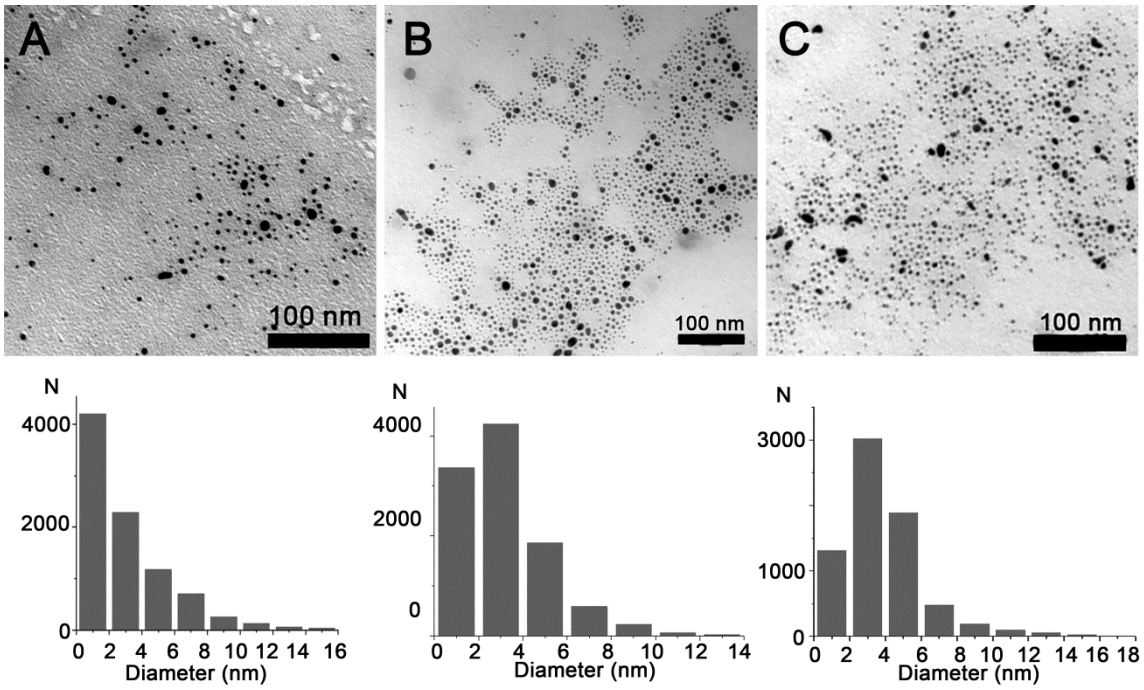

Figure 1. TEM image and size distribution histogram associated to a) **1aAuNP**, b) **1bAuNP**and c) **1cAuNP**.

Figure 1 shows TEM images and size distribution histograms of first generation heterofunctionalized AuNPs **1a-cAuNP**. The corresponding images for higher generation AuNPs are collected in Supporting Information (Figures S2-S7). The size of these AuNPs (TEM) was independent of dendron generation or dendron/PEG ratio, presenting diameters from 2 to 5 nm. These systems were stable under inert atmosphere, maintaining size and shape for over 18 months (Figure S8). It should be noted that stability of PEGylated AuNPs (**1-3,a-cAuNP**) was higher than non-PEGylated AuNPs (**1-3AuNP**), according with the stabilizing capacity of this kind of polymer.[61-63]

The hydrodynamic diameters of AuNPs in water solution were measured by DLS (Figures S9-S17). The higher diameters obtained by DLS, compared with those obtained by TEM, are related with the differences between both techniques. Whereas TEM only measures the metallic core, the size obtained by DLS would include ligands attached to the AuNPs and solvent layer at the interface. The polydispersity (PDI) and the diameter (d_z) obtained by DLS can be used to calculated a theoretical d_n value (Cd_n

= $d_z/(1+Q)^5$; where Q correspond with PDI).[37, 64, 65] These calculated diameters are closer to those measured by TEM. UV spectra also confirmed AuNPs formation, observing for all nanoparticles the band belonging to the surface plasmon resonance at about 520 nm (Figures S18-S20).

Functionalization of AuNPs was detected by TGA and ^{1}H-NMR spectroscopy. TGA gives information about the percentage of organic matter and inorganic matter in the AuNPs (Table 1, Table S1, Figures S21-29). In ^{1}H-NMR spectroscopy, the resonances of the different ligands on AuNP surface (**1-3,a-cAuNP**) were observed at similar chemical shifts than those of the starting dendrons (**I-III**)[37]and HS-PEG ligand (Figures S30-S38). The methylene groups closest to the gold surface CH_2SAu, corresponding with the focal point of dendrons and PEG derivative, were not observed due to their proximity to the gold surface. ^{1}H-NMR spectra also allowed calculation of final dendron/PEG molar ratio of heterofunctionalized AuNPs, using integrals of external methyl groups of trimethylammonium moieties of dendrons and methoxy group of PEG ligand (Table 1, Table S1). This final dendron/PEG ratio is clear dependent on the initial one and dendron generation, although PEG proportion on heterofunctionalized AuNPs **1-3,a-cAuNP** is always higher than that expected. This result can be attributed to the necessity to reduce charge repulsion between cationic dendrons.

It is important to note that introduction of PEG ligands entails a reduction of the density in the number of functions on NP surface (ammonium groups of dendrons and PEG ligands, Tables 1 and S1) with respect to non-PEGylated AuNP, except for **1a-cAuNP**, which is covered with 1G dendrons. This fact can be related with relative sizes of dendrons and PEG, but also with conformation of both ligands. While dendrons tend to separate as much as possible to avoid charge repulsion, PEG can fold its structure

covering higher nanoparticle surface. This assessment is supported by the low density value of PEG ligands on AuNP covered only with this type of ligand.

Comparison of Zeta potential values of heterofunctionalized AuNP **1-3,a-cAuNP** with cationic homofunctionalized AuNP **1-3AuNP** showed an important reduction of this value. Probably, this is consequence of the presence of lesser cationic dendrons on AuNPs surface and because PEG ligand can mask dendron charge.

AuNPs	Molar ratio Dendron/PEG		%L[b]	d_n[c]	d_z[d]	PDI[e]	Cd_n[f]	ρ (F/nm^2)[g]	ZP[h]
	Theoretical	Obtained[a]							
1AuNP	-	-	45.2	1.8	10.3	0.391	2.0	11.6	50.0
1aAuNP	3/1	1/2.0	51.7	3.2	39.8	0.409	7.2	12.6	29.1
1bAuNP	1/1	1/2.9	59.9	3.2	24.5	0.471	3.6	16.1	23.8
1cAuNP	1/3	1/5.4	55.3	3.9	21.5	0.570	2.3	14.4	23.6.
2AuNP	-	-	67.7	2.2	15.8	0.444	2.5	71.8	63.7
2aAuNP	3/1	1/1.5	67.6	3.7	34.0	0.540	3.9	36.8	44.9
2bAuNP	1/1	1.1/1	66.6	2.8	23.3	0.298	6.3	30.2	41.1
2cAuNP	1/3	1/6.4	62.3	4.8	94.3	0.233	4.4	26.0	34.9
3AuNP	-	-	84.2	2.0	22.1	0.611	2.0	159.8	59.6
3aAuNP	3/1	1.5/1	77.4	3.9	26.0	0.473	3.8	84.8	48.0
3bAuNP	1/1	1/2.7	75.6	5.0	23.9	0.400	4.4	75.3	54.8
3cAuNP	1/3	1/6.0	68.0	3.3	35.5	0.381	7.1	27.5	46.0
PEGAuNP	-	-	64.6	3.1	256.1	0.475	36.8	13.7	21.5

Table 1. Selected data of AuNPs. a) Molar ratio obtained by NMR (integration of resonances of methyl groups of trimethylammonium moieties of dendrons and methoxy group of PEG ligand. b) % Organic matter obtained by TGA, corresponding with dendron and PEG coating. c) Diameter (d_n, nm) obtained by TEM. d) Diameter (d_z. nm) obtained by DLS. e) Polydispersity index (PDI) obtained by DLS. f) Diameter calculated (Cd_n, nm): $Cd_n = d_z/(1+Q)^5$; Q corresponds with PDI.[65] g) Number of functions (F) per nm^2 on AuNP surface (dendrons: 2 F for 1G, 4 F for 2G, 8 F for 3G; PEG: 1 F), calculated from TEM diameter, NMR and TGA (see Table S1). h) Zeta potencial (mV). **1-3AuNP** were previously described.[37]

Biological assays

Haemolysis and Cytotoxicity. The haemolysis data showed (Figure 2 and S39) that erythrocytes were very tolerant toward AuNPs covered with PEG and 1G (**1a-cAuNP**) and 2G (**2a-cAuNP**) dendrons in all the concentrations measured at 2 h and 24 h. Particularly, PEGylated NPs **2a-cAuNP** produced haemolysis below 5% even at 100 µg/ml, whilst non-PEGylated NPs **2AuNP** reached 70% haemolysis at 30 µg/ml. For **3a-cAuNP**, with the biggest 3G dendron, haemolysis over 20% was surpassed for AuNPs with lower PEG proportions (**3a-bAuNP**) at concentrations above 50 µg/ml after 24 h but not at 2 h. On the other hand, for **3cAuNP**, with the highest PEG proportion, haemolysis was kept below 20% at all concentrations studied. These data highlight the relevance of PEGylation, since non-PEGylated AuNPs covered with 2G cationic dendrons **2AuNP** were as hemolytic as **3AuNP**.[37]

As eukaryotic model to study viability of non-PEGylated **1-3AuNP** and PEGylated **1-3,a-cAuNP**, HeLa cells were chosen (Figure 3). The general trend observed was an increase of viability for PEGylated AuNPs with respect to non-PEGylated AuNPs. This is mainly observerd for AuNPs covered with 2G and 3G dendrons, since viability of AuNPs stabilized with 1G dendrons was similar for the non-PEGylated and PEGyalted systems. Also, viability of AuNPs with higher generation dendrons improved with increasing amount of PEG ligands. Of all the systems studied, the data point out that PEGylation of AuNPs with second generation dendrons are the most benefited, being viability of **2bAuNP** at 70 ppm and of **2cAuNP** at 100 ppm clearly over 50%, whilst non-PEGylated **2-AuNP** at these concentrations were clearly toxic.

The low toxicity of gold core and the important influence of AuNPs substituyents on toxicity has been previously reported.[66] On the other hand, it is known that positive charged systems destabilize negative charged cell membranes.[43] Hence, both haemolytic

and cytotoxicity properties of these dendronized AuNPs mainly arise from the presence of the cationic dendrons. Moreover, zeta potential analysis showed a diminishing of this value for PEGylated AuNPs, which can be related with the lower toxicity of PEGylated systems. For example, we have observed that viability of a fully PEGylated AuNPs was clearly over 80% at 100 ppm (**PEGAuNP**, Figure 3). However, PEGylation is not always an innocuous procedure and it has been described that this process affects the morphology and function of red blood cells in the long run, although do not have noticeable effects for short periods of time.[67, 68]

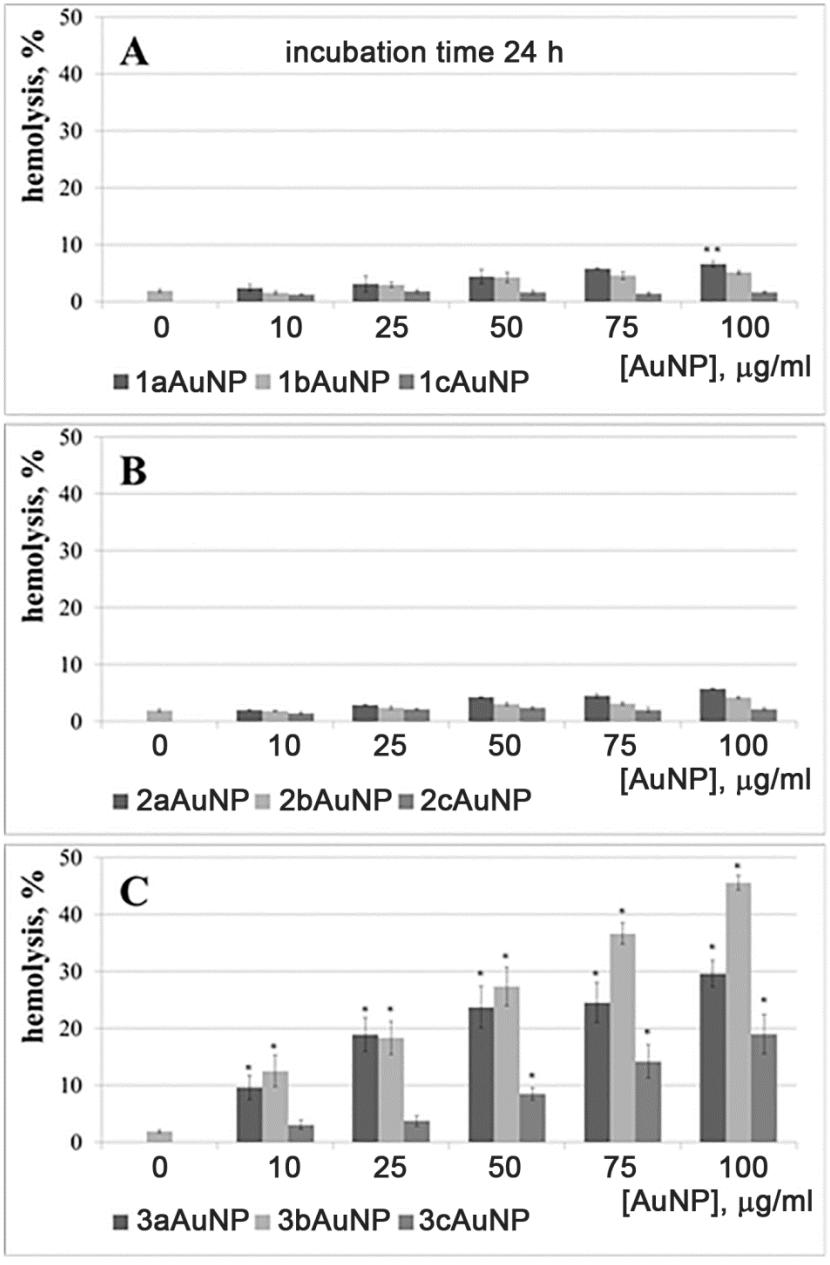

Figure 2. Extent of haemolysis after 24 h in the presence of PEGylated AuNPs decorated with dendrons: A) **1a-cAuNP**, B) **2a-cAuNP**, C) **3a-cAuNP**. Statistical significance of differences vs. control samples of blood erythrocytes alone (at *$p < 0.0002$, **$p < 0.01$) was estimated by the post-hoc Newman-Keuls test. Statistical significance between haemolysis rates within the group with different degrees of PEGylation with equal concentrations occurs in case of **3a-cAuNP** with all samples inside groups between each other ($p < 0.005$) except **3a**/**3b** at concentration of 25 μg/mL.

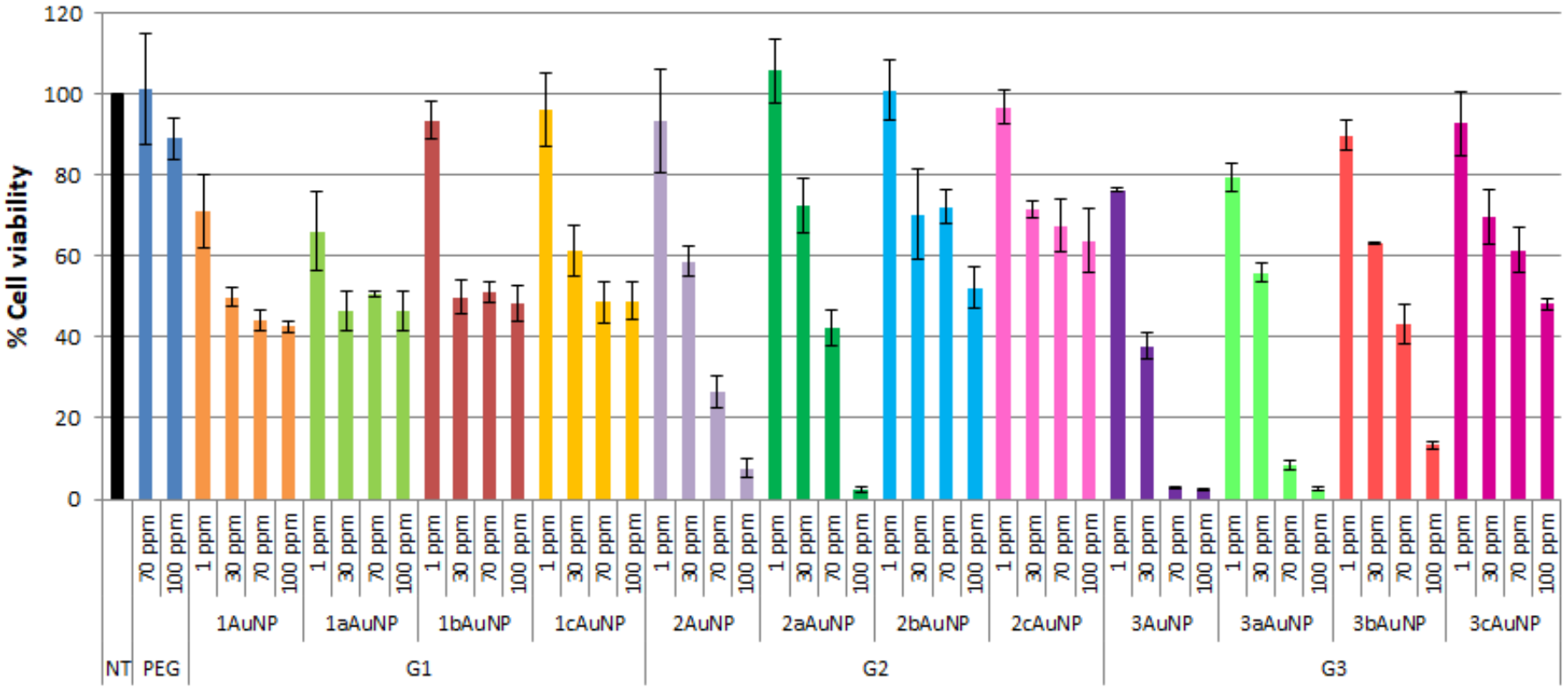

Figure 3. Cytotoxicity associated to homo and heterofunctionalized gold nanoparticles in Hela cells 24 h post-loading using MTT assay.

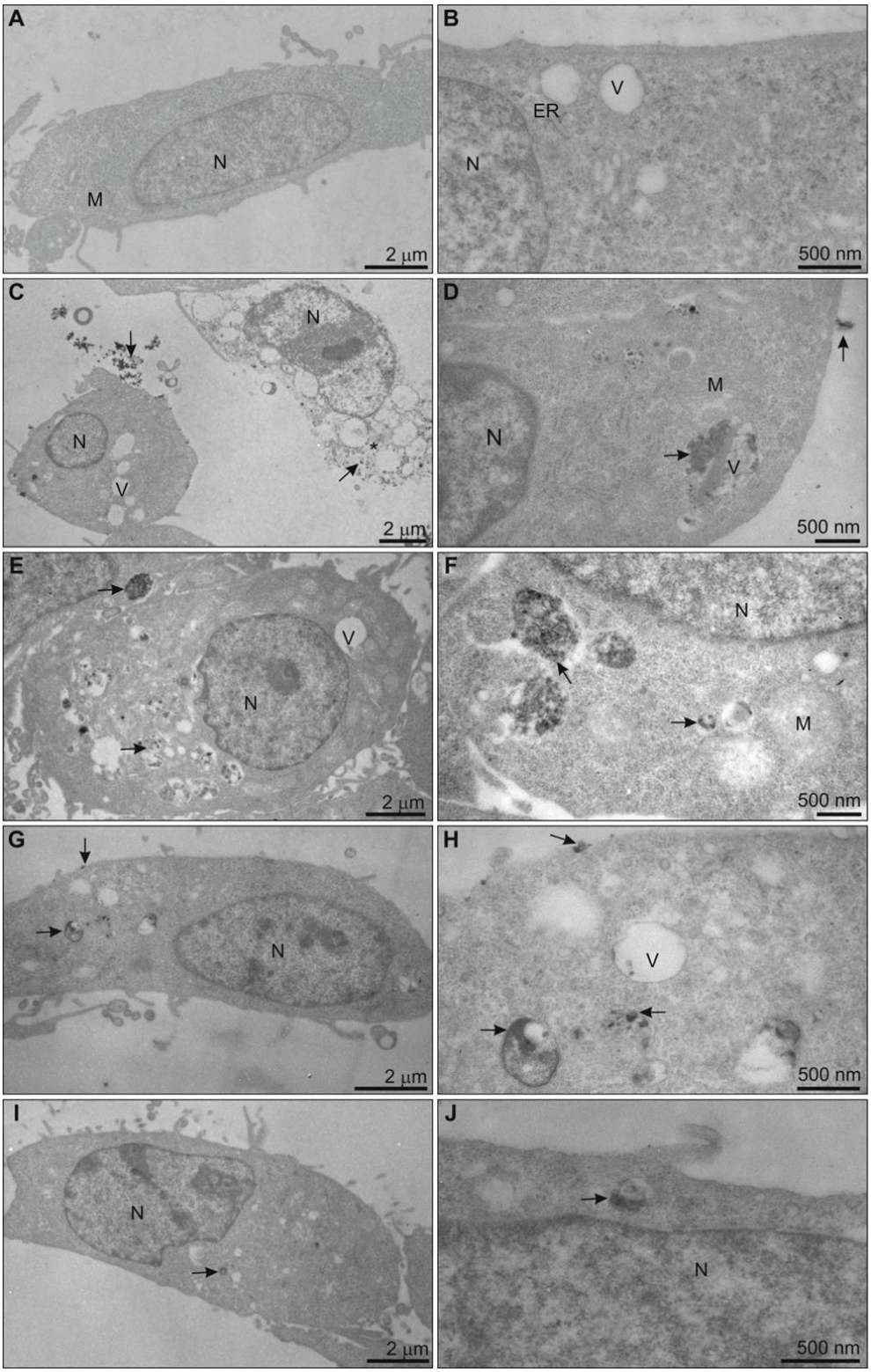

Figure 4. The ultrastructure of HeLa cells exposed to non-PEGylated 2AuNP and PEGylated 2a-cAuNP. A-B) control HeLa cell; C-D) 2AuNP (0.456 mg/ml); E-F) 2bAuNP; G-H) 2aAuNP; I-J) 2cAuNP. N – nucleus, M – mitochondrium, V – vesicle, ER – endoplasmic reticulum.

Ultrastructure of HeLa cells treated with PEGylated and non-PEGylated AuNPs. The ultrastructure of HeLa cells treated with **2AuNP** (Figure 4C-D) as well as **2a-cAuNP** (Figure 4E-J) was examined in relation to the untreated cells (Figure 4A-B). The control HeLa cells were spindle shaped and had a big oval nucleus (Figure 4A-B). The endoplasmic reticulum cisternae and mitochondria were visible within quite dense area of cytoplasm filled with ribosomes. Only single vesicles were noticed in the cytoplasm and they did not contain any electron-dense cargo (Figure 4A-B). The cells treated with non-PEGylated **2AuNP** changed their shape to more round and they were more vesiculated than control ones. The clusters of small electron dense granules were visible near cells (Figure 4C, arrows), adjusting their plasmalemma and in vesicles (Figure 4D, arrows). Such localization of AuNPs indicates endocytic pathway of uptake to cell.[69] Some cells growing in AuNP solution showed necrosis features: loss of plasma membrane integrity, swelling of the cytoplasm and disruption of the organelles (Figure 2C, asterisk).

Regarding HeLa treatment with PEGylated AuNPs, those treated with **2bAuNP** showed only a slightly changed ultrastructure. They were rather oval in shape and had round nucleus. Moreover, many vesicles with electron-dense cargo (Figure 2E-F, arrows) were visible in the area of cytoplasm indicating intensive uptake of **2bAuNP**.

The cells exposed to **2aAuNP** and **2cAuNP** had the same shape as control ones (Figures 2G, 2I). The only noticeable effect of **2aAuNP** treatment was cell vesiculation and the presence of the electron-dense material adjacent plasma membrane and inside endocytic vesicles (Figures 2G-H, arrows). However the amount of vesicles and electron-dense deposits was significantly lower than in the **2bAuNP** treated cells.

HeLa cells exposed to **2cAuNP**, with the highest PEG content, were characterised by the lowest vesiculation and rarely found electron-dense material (Figures 2I-J,

arrows). This result suggests that this PEGylated AuNPs hardly entered tested cells, probably due to the lower content of cationic dendron 2G on their surface.

As commented above, localization of AuNPs indicates endocytic pathway of internalization. The metal core, due to its size, should not fundamentally change the mechanism and then it should be similar to that of dendrimers. However, there is no universal method for endocytosis and it is highly dependent on the type of cells. These AuNPs can penetrate the cell through receptor-mediated mechanisms, namely, clathrin- and caveola-dependent endocytosis, although the possibility of macropinocytosis is not excluded.[70, 71]

Lymphocyte proliferation. T lymphocytes (T-cells) are cells that act as regulatory agents of the immune system, defending the body from foreign antigens such as viruses and fungi. T cell proliferation initiates the immune response. The *in vitro* lymphocyte proliferation assay is used to determine whether cells can divide after exposure to a suitable stimulus or not, as well as to compare the ability of several cell populations to divide in response to the same stimulus.[72] In order to determine if our systems constitute a non-specific antigen stimulus, the study of lymphocyte proliferation by **1-3,a-cAuNP** was carried out.

Peripheral blood mononuclear cells (PBMCs) were treated with PEGylated AuNPs (Figure 5). With the purpose of comparing these AuNPs with non-PEGylated (measured at 10 μM and 20 μM),[37] different concentrations were used for each generation: G1 (11 μg/mL, 22 μg/mL), G2 (15.2 μg/mL, 30.4 μg/mL), and G3 (25 μg/mL, 50 μg/mL). These concentrations in ppm for **1-3,a-cAuNP** corresponds with the molar concentration used for **1-3AuNP**. All considered AuNPs did not show antigenic effect (Figure 5) in given concentrations. Moreover, inhibition was observed in some cases.

Of all the NPs, **2aAuNP**, decorated with 2G dendrons and with the lowest PEG percentage, had clearly the strongest impact on lymphocyte proliferation (from 40% for 15.2 µg/mL to 10% for 30.4 µg/mL). In the case of the **2bAuNP**, the level of proliferation fell from 88.8% (15.2 µg/mL) to 51.3% (30.4 µg/mL). Similar toxicity was shown by **2cAuNP** at concentration of 15.2 µg/mL (85.5%) but slightly lower at a concentration of 30.4 µg/mL (79.4%). For these AuNPs, the results showed that the degree of PEGylation seems to play a substantial role in the activity, probably by reducing interaction with the cationic groups of dendrons.

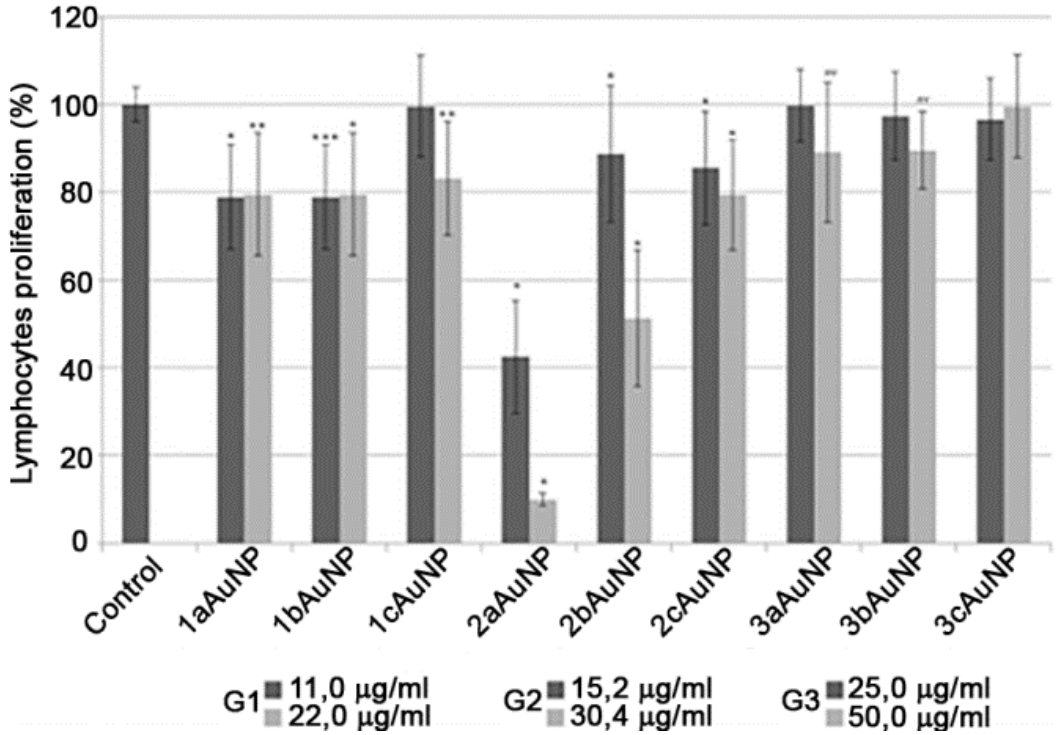

Figure 5. Extent of lymphocyte proliferation after 72 h in the presence of PEGylated gold nanoparticles **1-3,a-cAuNP**. Statistical significance of differences vs. control cells treated with PHA-M only (Phytohemagglutinin, M form) (at *p < 0.00005, **p < 0.0005, ***p < 0.003, ‴p < 0.03) was estimated by the post-hoc Newman-Keuls test.

Regarding AuNPs decorated with 1G dendrons **1aAuNP** and **1bAuNP**, they inhibited lymphocyte proliferation (about 20%) with no concentration dependence. In the case of the **1cAuNP**, with highest PEG percentage, at 11 µg/mL they had no effect

at all, while at 22 μg/mL proliferation was inhibited also about 20% (to 83.2%). Finally, **3a-cAuNPs** had the least impact on proliferation. The inhibition effect disappeared with increasing degree of PEGylation, as was observed at 50 μg/mL for **3cAuNP**.

Platelets aggregation. The parameters of platelet aggregation induced by AuNPs in platelet rich plasma were measured (Figure 6). The concentrations of AuNPs to study platelets aggregation were chosen from the data of haemotoxicity of these NPs. Two concentrations were finally chosen: 10 and 100 μg/mL.

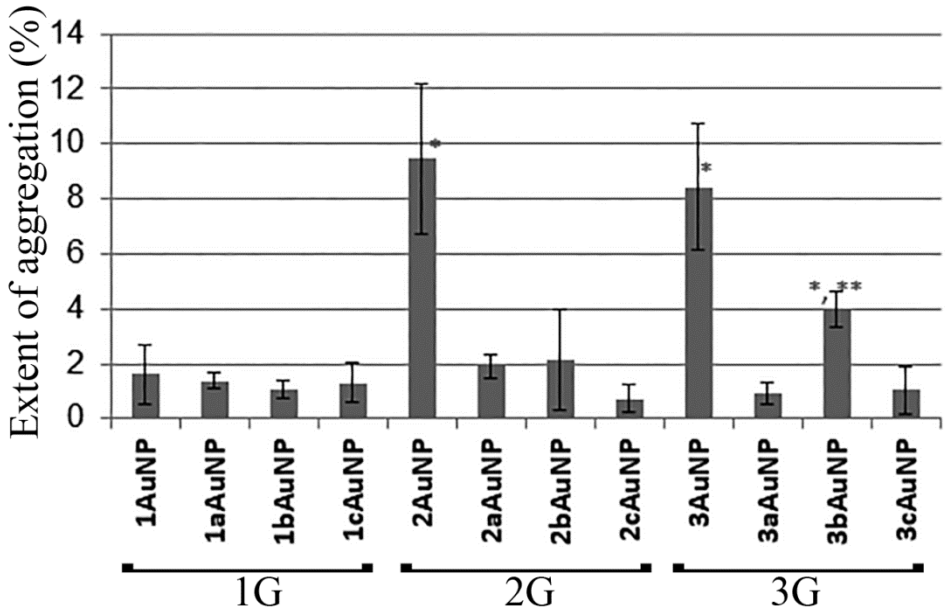

Figure 6. The extent in % of platelet aggregation induced by AuNPs in concentration of 100 μg/mL in platelet rich plasma (225000-230000 cells per μL). n = 6, mean+-S.D. * - $p < 0.05$ by ANOVA and post-hoc N-K test between (**1AuNP**, **2AuNP**, **3bAuNP**) and all other NP, ** - $p<0.05$ by ANOVA and post-hoc N-K test between **3bAuNP** and (**1AuNP**, **2AuNP**).

All studied AuNPs did not induce aggregation of platelets below 10 μg/mL (data not shown). At concentration of 100 μg/mL, PEGylated and non-PEGylated AuNPs differed in their effects, except for those covered with 1G dendrons. In these last cases, PEGylated **1a-cAuNP** and non-PEGylated **1AuNP** did not induce any effect on

platelets aggregation. In contrast, non-PEGylated AuNPs covered with 2G and 3G dendrons (**2AuNP**, **3AuNP**) significantly differed ($p < 0.05$) from PEGylated ones by their action on platelets. In general, PEGylated NPs **2a-cAuNP** and **3a-cAuNP** did not induce any effect on platelets aggregation, but **3bAuNP** (dendron/PEG = 1:1) that led to weak but statistically significant effect on aggregation of platelets. These data is in agreement with higher biocompatibility of PEGylated NPs.[73]

Previously has been reported that colloidal AuNPs practically do not cause platelet aggregation.[74] The level of aggregation is also low for non-PEGylated nanoparticles here discussed. In this case, dendrons are probably not conducive to increasing aggregation, unlike typical dendrimers, because dendrons have less degrees of freedom while on the surface of these rigid nanoparticles.[37] Thus, dendrons on AuNPs cannot spread over the platelet membrane reducing the interaction with receptors that are involved in aggregation.[75, 76]

Recognition of PEG with anti-PEG antibodies. PEGylation of biological and chemical compounds have many advantages such as good water solubility, lack of toxicity and low immunogenicity. However, long using PEGylated products lead to increase anti-PEG antibodies in blood. Thus, it is very important to check whether quantity of PEG chains and number and generation of dendrons attached to AuNPs have influence on PEG recognition by anti-PEG antibodies. To estimate the recognition of PEG attached to dendritic AuNPs, ELISA assays with anti-PEG antibodies were applied. These PEG-antibodies recognize the methyl group at the end of PEG chain.

On Figure 7, it can be observed that absorbance (optical density, OD) decreases in the presence of antibodies. The higher recognition by anti-PEG antibodies is observed for **2a-cAuNP**, with 2G dendrons. The lowest recognition is visible for dendritic **1a-cAuNP** and **3a-cAuNP**. Since anti-PEG antibodies recognize the methyl group at the

end of PEG chain, the more exposed PEG is, the higher recognition is observed. It seems that in **2a-cAuNP** PEG chains are more exposed and stretched due to the size of 2G dendrons, whilst in **3a-cAuNP** the bigger size of 3G dendrons hinder the interaction between antibodies and PEG. On the other hand, the PEG chain in **1a-cAuNP** containing the smallest 1G dendrons could be wrapped and therefore the end group of PEG chain would be less visible for antibodies.

On the other hand, we should expect that more PEG is attached to AuNPs surface, more antibodies can recognize these chains. However, the data point out that the higher recognition occurred for molar ratios 1:3 and 3:1 (dendron:PEG respectively). The lower recognition is for molar ratio 1:1. The explanation for the results is, probably, the nature of PEG chain alone. The PEG chain can be easily visible in presence of excess of dendrons (chain could be more stretched). With increasing PEG contain (molar ratio 1:1) the PEG is less visible because it could start to wrap around nanoparticles. In presence of excess of PEG, again PEG chains start to be more visible for antibodies. The above data suggest that recognition of PEGylated AuNPs depends on molar ratio between PEG and dendrons and on dendron generation.

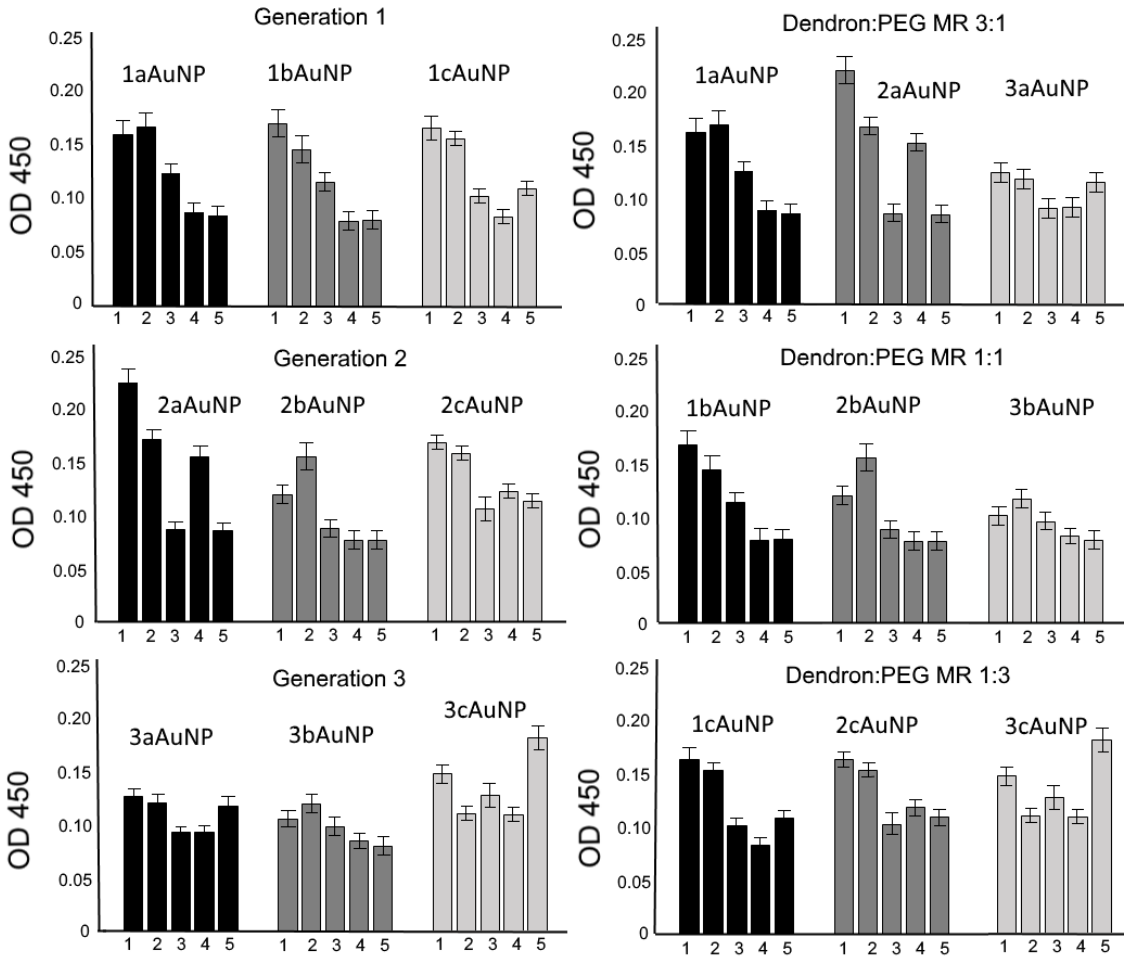

Figure 7. Direct ELISA antigen dose-response curve using anti-PEG antibodies. Antibodies concentration series: 1- 0.125 mg/ml, 2- 0.0625 mg/ml, 3- 0.0312 mg/ml, 4- 0.0156 mg/ml, 5- 0.0078 mg/ml. A HRP-conjugated goat anti-rabbit IgM (1/1000) was used as the secondary antibody.

CONCLUSIONS

One pot reaction of gold precursor with cationic carbosilane dendrons and PEG is an adequate procedure for the synthesis of AuNPs covered with both type of ligands. The final dendron/PEG ratio is mainly dependent on initial one, observing higher presence of PEG ligands on AuNPs due to charge repulsion between cationic dendrons. However, the dendron/PEG ratio does not affect size of AuNPs. The presence of PEG chains on these heterofunctionalized AuNPs diminish the overall positive charge,

particularly on those AuNPs covered with lower generation dendrons. This behavior is due to the relative length of the PEG ligand with respect to dendron size, which overlaps positive charge of the dendrons.

The presence of PEG on dendronized AuNPs reduces haemolysis, platelet aggregation and modification of ultrastructure of a model of eukaryotic cells (HeLa). The uptake of AuNPs by cells was higher for non-PEGylated AuNPs (**2AuNP**) and PEGylated (**2bAuNP**). In the particular case of AuNPs with the higher proportion of PEG, minimum proportion of cationic dendron, their uptake was negligible, confirming the necessity of cationic groups to penetrate cell membrane.

Dendron generation and dendron/PEG ratio have an important influence on interaction of AuNPs with anti-PEG antibodies. The higher recognition by antibodies is for **2a-cAuNP**, with 2G dendrons. These data point out that in these AuNPs, the terminal group of PEG, which is recognized by antibodies, is more exposed due to the size of 2G dendrons. In **3a-cAuNP**, covered with 3G dendrons, these dendrons hide PEG chain, whilst in **1a-cAuNP**, covered with 1G dendrons, the smaller size of dendrons favours PEG folding making the methoxy group less available for interaction with antibodies.

Hence, the dendron/PEG ratio and dendron generation (size) clearly alter properties of AuNPs. This fact can be the key to choose the suitable system for transfection. Research on this idea is now being in progress.

MATERIALS AND METHODS

General considerations

All reactions were carried out under inert atmosphere and solvents were purified from appropriate drying agents when necessary.Unless otherwise stated, reagents were

obtained from commercial sources and used as received. Compounds $HSG_n(S\text{-}NMe_3Cl)_m$ (where n = 1, m = 2; n = 2, m =4 ; n = 3, m = 8) were synthesized as published [37]. Thiol-ene reactions were carried out employing a HPK 125W Mercury Lamp from Heraeus Noblelight with maximum energy at 365 nm, in normal glassware under inert atmosphere. NMR spectra were recorded on a Varian Unity VXR-300 (300.13 (^{1}H)). Chemical shifts (δ) are given in ppm. ^{1}H resonances were measured relative to solvent peaks considering TMS = 0 ppm. UV-vis absorption was measured with a Perkin-Elmer Lambda 18 spectrophotometer. The spectra were recorder by measuring dilute samples in a quartz cell with a path length of 1 cm. Zeta potential and DLS were measured in a Zetasizer Nano ZS (Malvern Instruments Ltd., UK) at 25 ºC. Thermogravimetric analysis (TGA) were performed using a TGA Q500. Dry and pure samples (2-10 mg) were placed into platinum sample holder under nitrogen atmosphere. The measurements were recorded from 25 to 1000 ºC, with heating rate of 10 ºC/min.

Synthesis of compounds

A description of the synthesis of first generation AuNPs with the equal ratio HSG1(S-NMe_3Cl)/HS-PEG (**1bAuNP**) follows. The procedures and data of all compounds can be found in the Supporting information.

AuNP@PEG©(SG_1(S-NMe_3Cl)$_2$ ***(1bAuNP)***. A mix of aqueous solution (53.2 mL, 12.5 mM) of compound $HSG_1(S\text{-}NMe_3Cl)_2$ (0.30 mmol. 149 mg) and HS-PEG (Mn = 800, 0.30 mmol, 240 mg) was added dropwise to an aqueous solution of $HAuCl_4{\cdot}3H_2O$ (20 mL, 30 mM, 0.6 mmol, 236 mg). $NaBH_4$ in water (15 mL, 200 mM, 3 mmol, 116 mg) was added dropwise before, and the mixture stirred 4 h. AuNP were purified by dialysis (MWCO 20 kDa) yielding **1bAuNP** (238 mg).

Data for: NMR (D_2O): ^{1}H NMR: δ 0.01 (SiCH_3), 0.56 ($SCH_2CH_2CH_2CH_2Si$), 0.87 ($SiCH_2CH_2S$), 1.45 ($SCH_2CH_2CH_2CH_2Si$), 1.73 ($SCH_2CH_2CH_2CH_2Si$), 2.62

(SiCH_2CH_2S), 2.89 (SCH_2CH_2N), 3.04 (NCH_3), 3.24 (O*Me*, PEG), 3.32 (SCH_2CH_2N), 3.56 (OCH_2CH_2O, PEG)). Reactant molar ratio HSG_1(S-$NMe_3Cl)_2$/HS-PEG molar ratio= 1/1. Calc. molar ratio (NMR) HSG_1(S-$NMe_3Cl)_2$/HS-PEG= 1/2.9. TGA (%): Au, 40.1; L, 59.9. UV-vis: 500 nm. Zeta Potential (mV): 23.8. DLS (nm): 24.47. Mean diameter of silver core (TEM) = 3.2 nm.

Hemotoxicity

Blood from healthy donors, obtained from Central Blood Bank in Lodz, was anticoagulated with 3% sodium citrate. Erythrocytes separated from blood plasma and leukocytes by centrifugation (4000 g, 10 min) at 4°C were washed 3 times with PBS (phosphate buffered saline; pH = 7.4). Erythrocytes were used immediately after isolation. PEGylated **1-3-a-cAuNP** were added at 10, 25, 50, 75 and 100 µg/ml at a 2% hematocrit value and incubated at 37°C. After 2 h and 24 h, these incubated suspensions were centrifuged (1000 g, 10 min) and haemolysis determined by measuring the free hemoglobin content in the supernatant at 540 nm. The percentage haemolysis was calculated from the formula:

Haemolysis [%] = (A/Ac) x 100%

Where A is the absorbance of the sample, and Ac is the absorbance of the sample in water (100% haemolysis).

Transmission electron microscopy (TEM) of HeLa cells

Cells for TEM were fixed with 2.5% glutaraldehyde in 0.1 M PBS pH = 7.2 for 3 h at 4°C. Subsequently they were rinsed with the same buffer, scraped off and dispersed into 2 % agar. The material in the agar blocks was postfixed in 1% OsO_4 for 2 h at 4 C. Subsequently the material was dehydrated in a graded series of ethanol than propylene oxide and embedded in Epon-Spur's resin mixture. Sample resin blocks were sectioned on an Ultra Cut E (Reichert Jung, Germany) ultramicrotome with a diamond knife.

Ultrathin sections (60-70 nm) were placed on formvar coated nickel grids and stained with a uranyl acetate and lead citrate. The cell ultrastructure was examined in transmission electron microscope JEM 1010 (JEOL Ltd, Japan) at 80 kV. The developed films were scanned using Perfection V700 PHOTO scanner (Epson, Japan) at the resolution 1200 dpi.

Lymphocytes proliferation

Experiments were carried out on human lymphocytes, that isolated from whole blood of healthy donors.Lymphocytes were isolated using Histopaque 1077 in room temperature.

The cells were seeded at concentration $1x10^6$ cells/mL in 100 µL of full RPMI (10% FBS, 100 U/mL penicillin, 0.1 mg/ml streptomycin) on 96-well plates (100000 cells/well) and incubated at 37ºC in humidified atmosphere with 5% CO_2.

Effects of dendronized and PEGylated AuNPs were observed by cell treatment with concentrations with respect to 10 and 20 µM of non-PEGylated AuNPs.

The isolated cells were incubated 72 h in a humidified 37°C, 5% CO_2 incubator in the presence (test samples) or absence (control samples) of AuNPs, and in the presence or absence of phytohemagglutinin (PHA-M) to assess the inhibition or induction of proliferation, respectively. The final concentration of PHA-M was 10 µg/ml.

After 72h incubation, cytotoxicity was evaluated by Alamar Blue assay (with resazurin, 10 µg/ml). Fluorescence measurements were carried out on Fluoroscan Ascent FL at λ_{ex}=530 nm and λ_{em}=590 nm. Viability of cells (%) was calculated relatively to the control (20 µl of PBS added to the wells).

The degree of cell proliferation by AuNPs was calculated according to the formula:

$$Proliferation\ [\%] = \frac{A_{NP^+}}{A_{K^+}} \cdot 100\%$$

Where:

A_{den+} – absorbance of the samples treated with nanoparticle in the presence of PHA-M;

A_{K+} – absorbance of positive control.

The results are presented as mean ± standard deviation; N = 6. Data were analyzed by conducting an ANOVA test with post-hoc Newman-Keulstests.

Platelets aggregation

Blood from healthy donors (men, 25-35 years) was taken. Aggregation of platelets was studied in platelet rich plasma.[37] For this, blood with addition of 3.8% of sodium citrate was centrifuged at 360 g for 5 min, and erythrocytes and leukocytes were removed to obtain platelet rich plasma.[37] Concentration of platelets in platelet rich plasma was at 225000 - 230000 cells per μL. Aggregation of platelets was studied using an automatic aggregometer AP2110 (SOLAR, Belarus). In the assay, 400 μL of platelets rich plasma was added to a thermostated (37ºC) plastic tube at a final platelet concentration of 225000 - 230000 cells per μL.[37] AuNPs in two concentrations: 10 μg/mL and 100 μg/mL were then added to the platelet rich plasma to induce platelets aggregation. Data are expressed as mean ± S.D. of 6 independent experiments. Significance was assessed using the one-way analysis of variance (ANOVA) with the post-hoc Newman-Keuls multiple comparisons test.

Recognition of PEG with anti-PEG antibodies

Wells were coated with 0.01 mg/ml (100 μL/well) of each dendritic gold nanoparticles. AuNPs were diluted in bicarbonate coating buffer and incubated on the plate overnight at 4ºC. After that the plate was washed with PBS (containing 0.05% Tween20) 5 times and 150 μL of blocking buffer was added to each well. The plate was incubated for 1 h at 37ºC and then washed 4 times in wash buffer. After blocking step the anti-PEG antibodies (Abcam) were added (in concentration range from 0.125 mg/ml

to 0.0078 mg/ml in volume 100 µL) and samples were incubated for 1 h at 37ºC. Again, after this step the plate was washed 3 times in wash buffer. Then, 100 µL of horseradish peroxidase-conjugated secondary antibodies (diluted accordingly to company protocol) was added to each well and incubated for 1 h at 37ºC. After washing the 100 µL of OPD substrate solution (o-phenylenediamine dihydrochloride) was added to each well and incubated in room temperature for 30 min. After 30 min the stop solution (0.2 M H_2SO_4) was added and absorbance was measured at 450 nm.

SUPPORTING INFORMATION

Complete experimental section and methodology, synthesis of compounds, TEM images, NMR spectra.

CONFLICT OF INTEREST

The authors declare no conflict of interest.

ACKNOWLEDGMENTS

This work has been supported by grants from CTQ2017-86224-P (MINECO), SBPLY/17/180501/000358 (JCCM), consortiums NANODENDMED II-CM ref B2017/BMD-3703 and IMMUNOTHERCAN-CM B2017/BMD-3733 (CAM) to UAH. CIBER-BBN as an initiative funded by VI National R-D-i Plan 2008-2011, Iniciativa Ingenio 2010, Consolider Program, CIBER Actions and financed by the Instituto de Salud Carlos III with assistance from the European Regional Development Fund. Also the research was supported by project [NanoTENDO] by the National Science Centre, Poland under the M-ERA.NET 2, which has received funding from the European Union's Horizon 2020 research and innovation programme under grant agreement no

685451, partly supported by the Belarusian Republican Foundation for Fundamental Research and State Committee of Science and Technology of Belarus, grants B18TYUB-001, B18PLShG-004, by the Polish National Agency for Academic Exchange (NAWA), grant EUROPARTNER, No. PPI/APM/2018/1/00007/U/001. This article/publication is based upon work from COST Action CA 17140 "Cancer Nanomedicine from the Bench to the Bedside" supported by COST (European Cooperation in Science and Technology). The authors thank Dr.Łucja Balcerzak and Sylwia Michlewska for TEM technical assistance. A.B.-G. acknowledges MINECO for a predoctoral fellowship.

REFERENCES

1. C. Scholz, *Polymers for Biomedicine: Synthesis, Characterization, and Applications*, (2017) Wiley.
2. Y. J. Zhang, T. Sun and C. Jiang, Biomacromolecules as carriers in drug delivery and tissue engineering, *Acta Pharm. Sin. B*, **8** (2018) 34-50.
3. W. H. Tao and Z. G. He, ROS-responsive drug delivery systems for biomedical applications, *Asian J. Pharm. Sci.*, **13** (2018) 101-112.
4. Z. B. Li, E. Y. Ye, David, R. Lakshminarayanan and X. J. Loh, Recent Advances of Using Hybrid Nanocarriers in Remotely Controlled Therapeutic Delivery, *Small*, **12** (2016) 4782-4806.
5. I. A. Aljuffali, C. L. Fang, C. H. Chen and J. Y. Fang, Nanomedicine as a Strategy for Natural Compound Delivery to Prevent and Treat Cancers, *Curr. Pharm. Design*, **22** (2016) 4219-4231.
6. C. Van Bruggen, J. K. Hexum, Z. Tan, R. J. Dalai and T. M. Reineke, Nonviral Gene Delivery with Cationic Glycopolymers, *Acc. Chem. Res.*, **52** (2019) 1347-1358.
7. M. Rezaee, R. K. Oskuee, H. Nassirli and B. Malaekeh-Nikouei, Progress in the development of lipopolyplexes as efficient non-viral gene delivery systems, *J. Control. Release*, **236** (2016) 1-14.
8. A. Qadir, Y. G. Gao, P. Suryaji, Y. Tian, X. Lin, K. Dang, S. F. Jiang, Y. Li, Z. P. Miao and A. R. Qian, Non-Viral Delivery System and Targeted Bone Disease Therapy, *Int. J. Mol. Sci.*, **20** (2019) 565.
9. X. M. Ge, M. Y. Wei, S. N. He and W. E. Yuan, Advances of Non-Ionic Surfactant Vesicles (Niosomes) and Their Application in Drug Delivery, *Pharmaceutics*, **11** (2019) 55.
10. D. D. Zhang, J. M. Liu, Y. Y. Liu, M. Dang, G. Z. Fang and S. Wang, The Application of Nanoparticles in Drug Delivery, *Prog. Chem.*, **30** (2018) 1908-1919.
11. G. L. Huang and H. L. Huang, Application of dextran as nanoscale drug carriers, *Nanomedicine*, **13** (2018) 3149-3158.
12. W. K. Hu, M. Ying, S. M. Zhang and J. L. Wang, Poly(amino acid)-Based Carrier for Drug Delivery Systems, *J. Biomed. Nanotechnol.*, **14** (2018) 1359-1374.

13. A. Bernkop-Schnurch, Strategies to overcome the polycation dilemma in drug delivery, *Adv. Drug Deliv. Rev.*, **136** (2018) 62-72.
14. A. Lancelot, R. Clavería-Gimeno, A. Velázquez-Campoy, O. Abian, J. L. Serrano and T. Sierra, Nanostructures based on ammonium-terminated amphiphilic Janus dendrimers as camptothecin carriers with antiviral activity, *Eur Polym J*, **90** (2017) 136–149.
15. P. M. Levine, T. P. Carberry, J. M. Holub and K. Kirshenbaum, Crafting precise multivalent architectures, *MedChemComm*, **4** (2013) 493-509
16. M. Mammen, S.-K. Choi and G. M. Whitesides, Polyvalent Interactions in Biological Systems: Implications for Design and Use of Multivalent Ligands and Inhibitors, *Angew. Chem., Int. Ed.*, **37** (1998) 2754–2794.
17. J. Huskens, L. J. Prins, R. Haag and B. J. Ravoo, *Multivalency: Concepts, Research and Applications*, (2018) Wiley.
18. L. P. Zhou, Y. L. Shan, H. Hu, B. Yu and H. L. Cong, Synthesis and Biomedical Applications of Dendrimers, *Curr. Org. Chem.*, **22** (2018) 600-612.
19. A. Baeza, D. Ruiz-Molina and M. Vallet-Regi, Recent advances in porous nanoparticles for drug delivery in antitumoral applications: inorganic nanoparticles and nanoscale metal-organic frameworks, *Expert Opin. Drug Deliv.*, **14** (2017) 783-796.
20. N. Elahi, M. Kamali and M. Baghersad, Recent biomedical applications of gold nanoparticles: A review, *Talanta*, **184** (2018) 537-556.
21. H.-H. Jeong, E. Choi, E. Ellis and T.-C. Lee, Recent advances in gold nanoparticles for biomedical applications: from hybrid structures to multi-functionality, *J. Mat. Chem. B*, **7** (2019) 3480-3496.
22. F.-Y. Kong, J.-W. Zhang, R.-F. Li, Z.-X. Wang, W.-J. Wang and W. Wang, Unique Roles of Gold Nanoparticles in Drug Delivery, Targeting and Imaging Applications, *Molecules*, **22** (2017) 1445-1457.
23. C. M. McIntosh, E. A. Esposito, A. K. Boal, J. M. Simard, C. T. Martin and V. M. Rotello, Inhibition of DNA transcription using cationic mixed monolayer protected gold clusters, *J. Am. Chem. Soc.*, **123** (2001) 7626–7629.
24. Y. Hernández, R. González-Pastor, C. Belmar-Lóez, G. Mendoza, J. M. de la Fuente and P. Martín-Duque, Gold nanoparticle coatings as efficient adenovirus carriers to non-infectable stem cells, *RSC Adv.*, **9** (2019) 1327-1334.
25. A. Dinari, T. T. Moghadam, M. Abdollahi and M. Sadeghizadeh, Synthesis and Characterization of a Nano-Polyplex system of GNRs-PDMAEA-pDNA: An Inert Self-Catalyzed Degradable Carrier for Facile Gene Delivery, *Sci Rep*, **8** (2018) 8112.
26. G. R. Newkome, C. N. Moorefield and F. Vögtle, Dendrimers and Dendrons: Concepts, Syntheses, Applications, *Dendrimers and Dendrons: Concepts, Syntheses, Applications. Wiley-VCH, Weinheim, Germany.*, (2001).
27. O. Rolland, C. O. Turrin, A. M. Caminade and J. P. Majoral, Dendrimers and nanomedicine: multivalency in action, *New J. Chem.*, **33** (2009) 1809-1824.
28. P. Ortega, J. Sánchez-Nieves, M. Martínez-Bonet, A. J. Perisé-Barrios, R. Gómez, M. A. Muñoz-Fernández and F. J. de la Mata, Cationic Dendritic Systems as Non-viral Vehicles for Gene Delivery Applications, *Cationic Polymers in Regenerative Medicine, Cationic Dendritic Systems as Non-viral Vehicles for Gene Delivery Applications*, (2015) 321-355.
29. M. Sánchez-Milla, I. Pastor, M. Maly, M. J. Serramía, R. Gómez, J. Sánchez-Nieves, F. Ritort, M. A. Muñoz-Fernández and F. J. de la Mata, Study of non-covalent interactions on dendriplex formation: Influence of hydrophobic, electrostatic and hydrogen bonds interactions, *Colloid Surf. B-Biointerfaces*, **162** (2018) 380-388.
30. M. J. Serramía, S. Álvarez, E. Fuentes-Paniagua, M. I. Clemente, J. Sánchez-Nieves, R. Gómez, F. J. de la Mata and M. A. Muñoz-Fernández, In vivo delivery of siRNA to the brain by carbosilane dendrimer, *J. Control. Release*, **200** (2015) 60-70.

31. E. Fuentes-Paniagua, M. J. Serramía, J. Sánchez-Nieves, S. Álvarez, M. A. Muñoz-Fernández, R. Gómez and F. J. de la Mata, Fluorescein Labelled Cationic Carbosilane Dendritic Systems for Biological Studies, *Eur. Polym. J.*, **71** (2015) 61–72.
32. L. S. Mbatha and M. Singh, Starburst Poly(amidoamine) Dendrimer Grafted Gold Nanoparticles as a Scaffold for Folic Acid-Targeted Plasmid DNA Delivery In Vitro, *J. Nanosci. Nanotechnol.*, **19** (2019) 1959-1970.
33. P. Kesharwani, H. Choudhury, J. G. Meher, M. Pandey and B. Gorain, Dendrimer-entrapped gold nanoparticles as promising nanocarriers for anticancer therapeutics and imaging, *Prog. Mater. Sci.*, **103** (2019) 484-508.
34. T. J. Cho, R. A. Zangmeister, R. I. MacCuspie, A. K. Patri and V. A. Hackley, Newkome-type dendron stabilized gold nanoparticles: Synthesis, reactivity, and stability, *Chem. Mater.*, **23** (2011) 2665–2676.
35. C. E. Peña-González, P. García-Broncano, M. F. Ottaviani, M. Cangiotti, A. Fattori, M. Hierro-Oliva, M. L. González-Martín, J. Pérez-Serrano, R. Gómez, M. A. Muñoz-Fernández, J. Sánchez-Nieves and F. J. de la Mata, Dendronized Anionic Gold Nanoparticles: Synthesis, Characterization, and Antiviral Activity, *Chem. Eur. J.*, **22** (2016) 2987-2999.
36. X. J. Li and K. Kono, Functional dendrimer-gold nanoparticle hybrids for biomedical applications, *Polym. Int.*, **67** (2018) 840-852.
37. C. E. Peña-González, E. Pedziwiatr-Werbicka, D. Shcharbin, C. Guerrero-Beltrán, V. Abashkin, S. Loznikova, J. L. Jiménez, M. Á. Muñoz-Fernández, M. Bryszewska, R. Gómez, J. Sánchez-Nieves and F. J. de la Mata, Gold nanoparticles stabilized by cationic carbosilane dendrons: synthesis and biological properties, *Dalton Trans.*, **46** (2017) 8736-8745.
38. B. Xu, A. Li, X. Hao, R. Guo, X. Sh and X. Cao, PEGylated dendrimer-entrapped gold nanoparticles with low immunogenicity for targeted gene delivery, *RSC Adv.*, **8** (2018) 1265-1273.
39. P. Wang, X. Wang, L. Wang, X. Hou, W. Liu and C. Chen, Interaction of gold nanoparticles with proteins and cells, *Sci. Technol. Adv. Mater.*, **16** (2015) 034610.
40. F. Ilaria, V. Iole, C. Cesare and V. Russo., The puzzle of toxicity of gold nanoparticles. The case-study of HeLa cells., *Toxicol. Res.*, **4** (2015) 796-800.
41. D. Shcharbin, E. Pedziwiatr and MariaBryszewska, How to study dendriplexes I: Characterization, *J. Control. Release*, **135** (2009) 186-197.
42. D. Shcharbin, E. Pedziwiatr, J. Blasiak and MariaBryszewska, How to study dendriplexes I: How to study dendriplexes II: Transfection and cytotoxicity, *J. Control. Release*, **141** (2010) 110-127.
43. R. Kircheis, S. Schuller, S. Brunner, M. Ogris, K. H. Heider, W. Zauner and E. Wagner, Polycation-based DNA complexes for tumor-targeted gene delivery in vivo, *J. Gene. Med.*, **1** (1999) 111-120.
44. M. Muthiah, I.-K. Park and C.-S. Cho, Surface modification of iron oxide nanoparticles by biocompatiblepolymers for tissue imaging and targeting, *Biotech. Adv.*, **31** (2013) 1224–1236.
45. Z. Amoozgar and Y. Yeo, Recent advances in stealth coating of nanoparticle drug delivery systems, *Wiley Interdiscip Rev Nanomed Nanobiotechnol*, **4** (2012) 219-233.
46. A. A. D'souza and R. Shegokar, Polyethylene glycol (PEG): a versatile polymer for pharmaceutical applications, *Expert Opin Drug Deliv*, **13** (2016) 1257-1275.
47. Y. J. Wang and C. Wu, Site-Specific Conjugation of Polymers to Proteins, *Biomacromolecules*, **19** (2018) 1804-1825.
48. J. Sánchez-Nieves, P. Fransen, D. Pulido, R. Lorente, M. A. Muñoz-Fernández, F. Albericio, M. Royo, R. Gómez and E. J. de la Mata, Amphiphilic Cationic Carbosilane-PEG Dendrimers: Synthesis and Applications in Gene Therapy, *Eur. J. Med. Chem.*, **76** (2014) 43-52.

49. F. M. Veronese and G. Pasut, PEGylation, successful approach to drug delivery, *Drug Discov. Today*, **10** (2005) 1451-1458.
50. Q. Yang and S. K. Lai, Anti-PEG immunity: emergence, characteristics, and unaddressed questions, *WIREs Nanomed. Nanobiotech.*, **7** (2015) 655-677.
51. D. Kim, H. El-Shall, D. Dennis and T. Morey, Interaction of PLGA nanoparticles with human blood constituents, *Colloids Surf. B*, **40** (2005) 83-91.
52. A. Barrios-Gumiel, J. Sanchez-Nieves, J. Pérez-Serrano, R. Gómez and F. J. d. l. Mata, PEGylated AgNP covered with cationic carbosilane dendrons to enhance antibacterial and inhibition of biofilm properties, *Int. J. Pharm.*, **569** (2019) 118591.
53. S. Thakur, P. Kesharwania, R. K.Tekade and N. K.Jain, Impact of pegylation on biopharmaceutical properties of dendrimers, *Polymer*, **59** (2015) 67-92.
54. S. P. Boulos, T. A. Davis, J. A. Yang, S. E. Lohse, A. M. Alkilany, L. A. Holland and C. J. Murphy, Nanoparticle-protein interactions: a thermodynamic and kinetic study of the adsorption of bovine serum albumin to gold nanoparticle surfaces, *Langmuir*, **29** (2013) 14984–14996.
55. W. Xiao, J. Xiong, S. Zhang, Y. Xiong, H. Zhang and H. Gao, Influence of ligands property and particle size of gold nanoparticles on the protein adsorption and corresponding targeting ability., *Int. J. Pharm.*, **538** (2018) 105–111.
56. L. Kennard, K. Rutkowski, R. Mirakian and A. Wagner, Polyethylene Glycol: Not Just a Harmless Excipient, *J Aller Cl Imm-Pract*, **6** (2018) 2173-2173.
57. E. C. Wenande, P. S. Skov, H. Mosbech, L. K. Poulsen and L. H. Garvey, Inhibition of polyethylene glycol–induced histamine release by monomeric ethylene and diethylene glycol: A case of probable polyethylene glycol allergy, *J Allergy Cl Imm*, **131** (2013) 1425–1427.
58. P. Zhang, F. Sun, S. Liu and S. Jiang, Anti-PEG antibodies in the clinic: current issues and beyond PEGylation, *J Control Release*, **244** (2016) 184–193.
59. Y. Fang, J. Xue, S. Gao, A. Lu, D. Yang, H. Jiang, Y. He and K. Shi, Cleavable PEGylation: a strategy for overcoming the "PEG dilemma" in efficient drug delivery, *Drug Delivery*, **24** (2017) 22-32.
60. N. M. Gulati, P. L. Stewart and N. F. Steinmetz, Bioinspired Shielding Strategies for Nanoparticle Drug Delivery Applications, *Mol Pharm*, **15** (2018) 2900-2909.
61. C. Díaz-Cruz, G. Alonso Núñez, H. Espinoza-Gómez and L. Z. Flores-López, Effect of molecular weight of PEG or PVA as reducing-stabilizing agent in the green synthesis of silver-nanoparticles, *Eur. Polym. J.*, **83** (2016) 265-277.
62. M. Popa, T. Pradell, D. Crespo and J. M. Calderón-Moreno, Stable silver colloidal dispersions using short chain polyethylene glycol, *Coll. Surf. A*, **303** (2007) 184-190.
63. X. Li and J. J. Lenhart, Aggregation and Dissolution of Silver Nanoparticles in Natural Surface Water, *Environ. Sci.Tech.*, **46** (2012) 5378-5386.
64. T. J. Cho, R. I. MacCuspie, J. Gigault, J. M. Gorham, J. T. Elliott and V. A. Hackley, Highly Stable Positively Charged Dendron-Encapsulated Gold Nanoparticles, *Langmuir*, **30** (2014) 3883-3893.
65. L. H. Hanus and H. J. Ploehn, Conversion of Intensity-Averaged Photon Correlation Spectroscopy Measurements to Number-Averaged Particle Size Distributions. 1. Theoretical Development, *Langmuir*, **15** (1999) 3091-3100.
66. E. E. Connor, J. Mwamuka, A. Gole, C. J. Murphy and M. D. Wyatt, Gold Nanoparticles Are Taken Up by Human Cells but Do Not Cause Acute Cytotoxicity, *Small*, **1** (2005) 325 –327.
67. T. Mocan, Hemolysis as Expression of Nanoparticles-Induced Cytotoxicity in Red Blood Cells, *Biotech. Molecular Biol. and Nanomed.*, **1** (2013) 7-12.
68. Z. He, J. Liu and L. Du, The unexpected effect of PEGylated gold nanoparticles on the primary function of erythrocytes, *Nanoscale*, **15** (2014) 9017-9024.

69. K. Solarska-Ściuk, A. Gajewska, S. Glińska, M. Studzian, S. Michlewska, Ł. Balcerzak, J. Skolimowski, B. Kolago and G. Bartosz, Intracellular transport of nanodiamond particles in human endothelial and epithelial cells, *Chem.-Biol. Interact.*, **219** (2014) 90–100.
70. M. Morille, C. Passirani, A. Vonarbourg, A. Clavreul and J.-P. Benoit, Progress in developing cationic vectors for non-viral systemic gene therapy against cancer, *Biomaterials*, **24-25** (2008) 3477-3496.
71. S. D. Conner and S. L. Schmid, Regulated portals of entry into the cell, *Nature*, **422** (2003) 37–44.
72. S. Romagnani, Regulation of the T cell response, *Clin. Exp. Allergy*, **36** (2006) 1357–1366.
73. M. J. Santos-Martínez, K. Rahme, J. J. Corbalán, C. Faulkner, J. D. Holmes, L. Tajber, C. Medina and M. W. Radomski, Pegylation Increases Platelet Biocompatibility of Gold Nanoparticles, *J. Biomed. Nanotech.*, **10** (2014) 1004-1015.
74. M. A. Dobrovolskaia, A. K. Patri, J. Zheng, J. D. Clogston, N. Ayub, P. Aggarwal, B. W. Neun, J. B. Hall and S. E. McNeil, Interaction of colloidal gold nanoparticles with human blood: effects on particle size and analysis of plasma protein binding profiles, *Nanomedicine*, **5** (2009) 106–117.
75. T. H. F. Thake, J. R. Webb, A. Nash, J. Z. Rappoport and R. Notman, Permeation of Polystyrene Nanoparticles across Model Lipid Bilayer Membranes, *Soft Matter.*, **9** (2013) 10265-10274.
76. N. A. Licata and A. V. Tkachenko, Kinetic Limitations of Cooperativity-Based Drug Delivery Systems, *Phys. Rev. Lett.*, **100** (2008) 158102.